Scientific Reports

https://doi.org/10.1038/s41598-026-35116-1

Article in Press

Comparison of the properties of nanopaper from chitin nanofibers prepared by mechanical and TEMPO-oxidized methods

Received: 21 August 2025

Accepted: 2 January 2026

Published online: 17 January 2026

Cite this article as: Mohammadlou A., Dehghani Firouzabadi M. & Yousefi H. Comparison of the properties of nanopaper from chitin nanofibers prepared by mechanical and TEMPO-oxidized methods. *Sci Rep* (2026). https://doi.org/10.1038/s41598-026-35116-1

Alireza Mohammadlou, Mohammadreza Dehghani Firouzabadi & Hossein Yousefi

Title page

Comparison of the properties of nanopaper from chitin nanofibers prepared by mechanical and TEMPO-oxidized methods

Alireza Mohammadlou [a], Mohammadreza Dehghani Firouzabadi [a*], Hossein Yousefi [b]

[a] *Department of Paper Science and Engineering, Gorgan University of Agricultural Sciences and Natural Resources, Gorgan, Iran.*
[b] *Laboratory of Sustainable Nanomaterials, Department of Wood Engineering and Technology, Gorgan University of Agricultural Sciences and Natural Resources, Gorgan, Iran.*

Corresponding Author:
Mohammadreza Dehghani Firouzabadi (□)
Tel.: +98-17-32427050
P.O. Box: 4918943464
Mobile phone: +98-912-2044207
E-mail: mdehghani@gau.ac.ir

Abstract

This study compares the structural, optical, and mechanical characteristics of chitin nanopapers fabricated through mechanical fibrillation and TEMPO-mediated oxidation. The TEMPO-oxidized nanopaper exhibited higher optical transparency (approximately 92%) than the mechanically fibrillated sample (around 60%), primarily due to enhanced nanofiber dispersion and smaller fibril diameters. In contrast, the mechanically produced nanopaper showed greater crystallinity (above 90%) and stronger hydrogen bonding, resulting in higher tensile strength and Young's modulus compared with the oxidized counterpart. Microscopic analyses confirmed the more homogeneous and well-dispersed network in TEMPO-treated samples, while spectroscopic results indicated the presence of carboxylate groups introduced by oxidation. The research overall highlights the usability of both nanopaper types in different applications and how TEMPO-oxidized nanopaper fits best under transparent and biodegradable packaging and mechanically treated nanopaper in applications requiring more strength.

Keywords:
Nanochitin, TEMPO-oxidation, Mechanical properties, Nanopapers, Optical transparency.

1. Introduction

The global seafood industry generates a substantial amount of waste, particularly from the processing of crustaceans such as shrimp and crabs, leading to significant environmental concerns [1,2]. Each year, millions of tons of chitin-containing shellfish waste are discarded, mostly resulting in waste and pollution [3,4]. In the sustainability and circular economy, chitin valorization as a green and functional biomaterial is a viable path forward [5]. A more efficient application of chitin to produce high-sustainability products not only reduces wastage of raw materials, but also adds to economic production whilst maximizing the crude materials, turning waste into high-grade materials [6-8]. This method is in line with worldwide initiatives to decrease waste and make greener alternatives a priority, and cements the promise of chitin as a key material in future eco-friendly technologies [9,10].

Chitin, the second most abundant biopolymer after cellulose in nature, has drawn much attention for its excellent physicochemical properties such as biocompatibility, biodegradability, and antimicrobial activity [3].

Chitin, derived from crustacean exoskeletons and fungal cell walls, possesses a hierarchical structure that can be broken down into nanoscale fibers using various processing strategies. Among these, top-down approaches such as mechanical fibrillation [11] and TEMPO (2,2,6,6-tetramethylpiperidine-1-oxyl)-mediated oxidation [12] are the most widely used for producing chitin nanofibers. Unlike these methods, electrospinning is primarily a down-top approache technique applied to chitin or its derivatives in solution form and is less common for producting individual nanofibrils from bulk chitin [13]. Mechanical processing can serve to physically separate the chitin fibrils in the absence of significant chemical transformation [11], whilst TEMPO oxidation leads to the introduction of carboxylated groups at the surface of the nanofibers, which give rise to altered dispersion characteristics, charge properties, and inherent reactivity [12,14-16].

Nanopaper is a high-density, flexible sheet made up of interwoven nanofibers that has become an attractive, sustainable alternative to regular paper because of its enhanced mechanical strength and gas barrier characteristics, along with adjustable surface chemistry [17-19]. The properties of chitin nanopaper greatly depend on the particular processing route used to extract the nanofibers [11,20]. The chitin nanofiber obtained through mechanical disintegration maintains the original chitin structure, with a reduced surface charge and a higher intrinsic crystallinity. Conversely, TEMPO-oxidized chitin nanofiber has more dispersed and higher colloidal stability due to their negatively charged surfaces, which can considerably influence the formation, density, and mechanical integrity of the nanopaper. The extent to which these processing methods influence the final chitin

nanopaper properties remains an unanswered question and must be examined through a comprehensive analysis.

Although extensive research has been conducted on chitin nanofibrils obtained through mechanical fibrillation and TEMPO-mediated oxidation, the underlying mechanisms linking these processing routes to the resultant nanopaper properties remain insufficiently understood. The novelty of this work lies in the systematic, side-by-side comparison of these two major top-down approaches using identical chitin sources under controlled conditions to isolate the influence of surface chemistry, fibril morphology, and inter-fibrillar interactions on the mechanical strength, porosity, and water resistance of the resulting nanopapers. Unlike previous studies that examined either mechanical disintegration or chemical oxidation independently, this study integrates both processes (Fig. 1) within a unified experimental framework and provides quantitative correlations between processing parameters and functional performance. Furthermore, by combining morphological, physicochemical, and barrier analyses, this research establishes a clearer structure property relationship that advances the rational design of chitin-based nanopapers for sustainable packaging and coating applications.

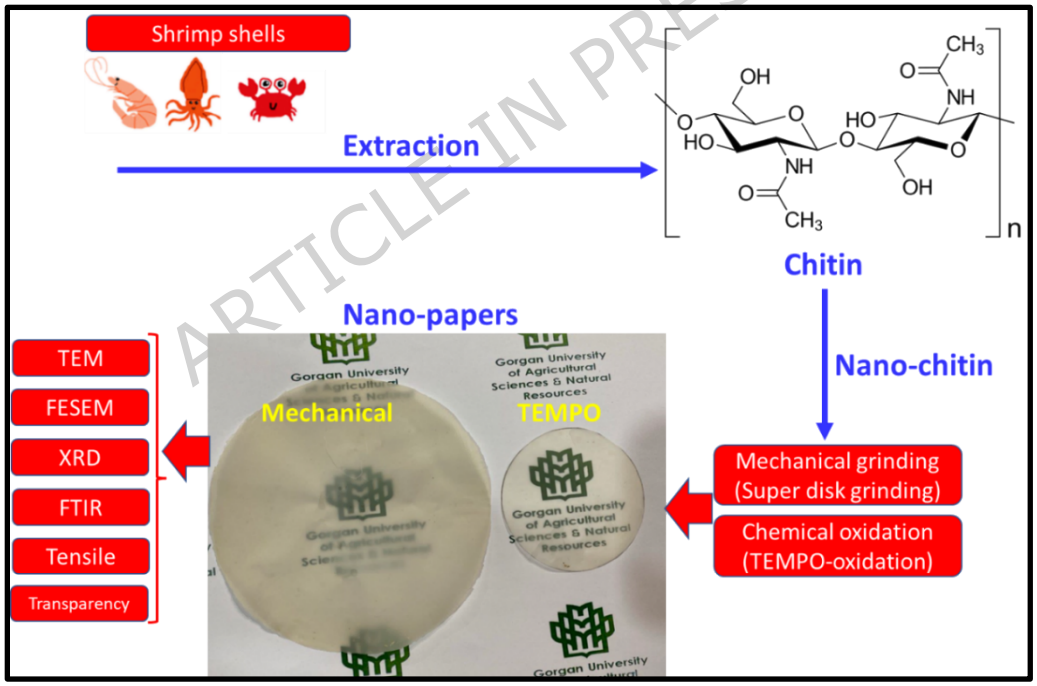

Fig. 1. Schematic of the research steps in this study.

2. Materials and methods

2.1. Raw materials

Chitin nanofibers with different surface morphologies were produced by using mechanical grinding and a chemical oxidation (TEMPO-oxidation) process. The mechanical treatment was performed using bleached dry chitin (extracted from shrimp shells, supplied by Nano Novin Polymer Co. (Gorgan,

Iran), 50 g of which was ground 3 times in a super disk grinding (Masuko MKCA6-2, Japan) to obtain well-dispersed chitin nanofibers at the speed of rotation of 1800 rpm. In the chemical process, 0.16 g of TEMPO was dissolved in 1 L of deionized water and stirred for 24 h; thereupon, 1.0 g of sodium bromide was added, and the stirring continued for 1 h. Then, 10 g of bleached dry chitin was added to the solution, and then sodium hypochlorite was slowly added until the pH was brought to the value of 10. To ensure the oxidation reaction proceeds continuously, reducing the processing error, the pH was maintained at 10-11 for 6 h. The obtained gel was washed with deionized water 3 times (500 mesh polyester filter bags to eliminate residual chemicals). It was finally passed through the disk grinding to get uniform TEMPO-oxidized chitin nanofibers.

2.2. Nanopaper preparation

For the preparation of 60 g/m^2 chitin nanopaper samples, an appropriate amount of each chitin nanofiber gel, including mechanically processed and TEMPO-oxidized variants, was weighed separately. For uniform dispersion, each suspension was stirred for 15 min at room temperature with a magnetic stir plate set at 250 rpm. A prepared suspension was poured onto a vacuum filtration system equipped with a 500-mesh (12 cm diameter) polyester filter. Removing water from the suspension with a vacuum pressure of 0.5 MPa resulted in the generation of a primary wet film. After dewatering, the as-prepared films were subjected to drying in a vacuum oven at 70 °C for 15 h between two pieces of glass plates to ensure sediment formation of nanopaper and provide enough structural stability.

2.3. Characterization

2.3.1. Transmission electron microscope (TEM)

The specimens were vacuum-dried and gold-coated before TEM examination. The nanopaper specimens were investigated by a TEM (CM 120) with an accelerating voltage of between 1.5 and 5 kV. Additionally, the average diameter of 100 fibers was determined utilizing digimizer image software (v. 4.1.1.0).

2.3.2. Field emission scanning electron microscopy (FESEM)

FESEM was used to evaluate the sample morphology. The samples were coated with a layer of platinum <0.2 nm thick, in a vacuum environment using a sputter coater machine. Finally, the coated samples were characterized by FESEM (Zeiss Sigma 300-HV, Germany) using an accelerating voltage of 5.0 kV.

2.3.3. X-ray diffraction (XRD)

X-ray Diffraction (XRD) is a widely utilized method for assessing the crystallinity index [21]. In this study, an XRD diffractometer (D8-Advance Bruker Cu Kα1, Germany) was employed to expose the samples to Cu-Kα radiation under operating conditions of 50 kV and 30 mA. The X-ray analysis

was conducted with a step size of 0.02°, and the scanning range was set between 10° and 60° (2θ). The crystallinity index of samples was calculated using Eq. 1.

$$CrI\ (\%) = [(I_{200}-I_{am}) / I_{200}] \times 100 \quad (1)$$

where I_{200} was the maximum intensity of the [200] lattice diffraction, which is typically in the range 2θ = 21°-23° and I_{am} was the intensity diffraction at 2θ = 18°

2.3.4. Fourier transform infrared (FTIR) spectroscopy

FTIR is an analytical tool used to determine the adventitious or attributable chemistry of materials by the way the materials absorb IR light at their distances. Films were investigated for their functional groups and the chemical change features by FTIR spectrometers (Perkin-Elmer, Spectrum RX I). Spectra were acquired from 4000 to 500 cm^{-1} (64 scans at 4 cm^{-1} resolution) [22].

2.3.5. Optical transparency

Optical transparency was evaluated through both quantitative and qualitative methods using a double-beam UV–vis spectrophotometer (U-2000, Hitachi Ltd., Japan) for precise measurements and a digital camera for visual assessment.

2.3.6. Mechanical properties

The tensile properties were evaluated following the ASTM D882-18 standard using a SANTAM universal tensile machine (model STM-1, Santam Co., Tehran, Iran) equipped with a 1 kN load cell and a cross-head speed of 10 mm/min. Samples were prepared in standard dimensions and secured between the tensile grips. Before testing, three specimens from each sample were conditioned at 30 °C and 50% relative humidity for 24 h. The reported tensile parameters included tensile strength and elongation at break.

2.4. Statistical analysis

All measurements were performed in triplicate, and the results are reported as mean ± standard deviation (n = 3). Statistical variability was evaluated using descriptive statistics, and error bars representing standard deviation were included in the corresponding figures to ensure data reliability.

3. Results and discussion

3.1. Morphology

The TEM micrographs and the corresponding diameter distributions of nanochitin obtained from mechanically processed chitin nanofibers and TEMPO-oxidized processes are presented in Fig. 2. The TEM micrographs are primarily used to illustrate the overall fibrillar morphology and network structure rather than to provide high-precision measurements of individual

fibril diameters. As shown in Fig. 2a, the mechanically processed nanofibers form an entangled and partially aggregated network, within which individual fibrils are not always clearly distinguishable. Accordingly, the reported average diameter of 26.04 ± 8.57 nm is derived from representative measurable regions, while acknowledging the inherent uncertainty caused by fibril overlapping and limited contrast at this magnification. This behavior can be attributed to the disk grinding process and the absence of sufficient electrostatic repulsion to achieve complete fibril separation, resulting in non-uniformity and aggregation consistent with the previous report [23]. In contrast, Fig. 2b demonstrates that TEMPO-oxidized chitin nanofibers exhibit a more homogeneous and finer fibrillar structure, with an average diameter of 7.72 ± 2.23 nm, reflecting the effectiveness of surface oxidation in promoting fibril individualization, while it is emphasized that quantitative diameter values are interpreted cautiously and supported by statistical analysis, and the TEM observations mainly serve to qualitatively confirm the morphological differences and fibrillar network characteristics between the two processing routes in accordance with the resolving capability of the presented images. Although TEMPO-mediated oxidation generally enhances fibril dispersion due to the introduction of negatively charged carboxylate groups, some degree of aggregation can still occur. This is primarily attributed to charge screening and partial re-association of nanofibrils during the drying stage, especially when residual counterions (e.g., Na^+) and hydrogen bonding forces reduce electrostatic repulsion between oxidized fibrils. Moreover, an excessively high degree of oxidation may lead to localized fibril damage, generating shorter fragments that tend to cluster through secondary interactions.

FESEM micrographs show that the morphology of the nanostructures used is in the form of fibers, so they are one-dimensional nanostructures; that is, two of their dimensions are in the nanoscale and one of their dimensions (length) is in the non-nanometric scale (more than 5 μm) (Fig. 3). The TEMPO-oxidized nanofiber structure, owing to the generation of carboxylate groups on its surface, is highly dispersed and uniform, offering greater clarity and homogeneity compared to mechanically processed nanofibers; moreover, the reduced diameter of the TEMPO-oxidized nanofibers results in a higher specific surface area, which is particularly significant for applications such as drug delivery and biosensors.

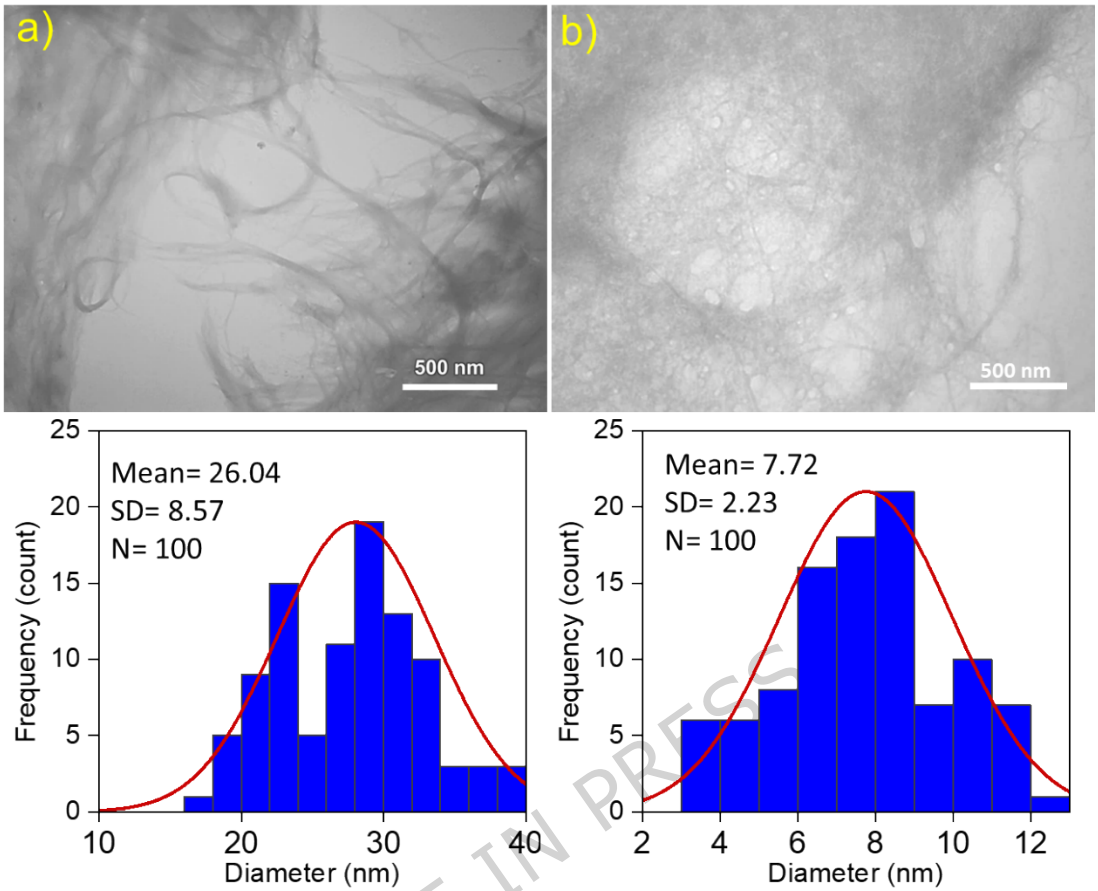

Fig. 2. TEM micrographs and diameter distribution of nanochitin of a) mechanical and b) TEMPO.

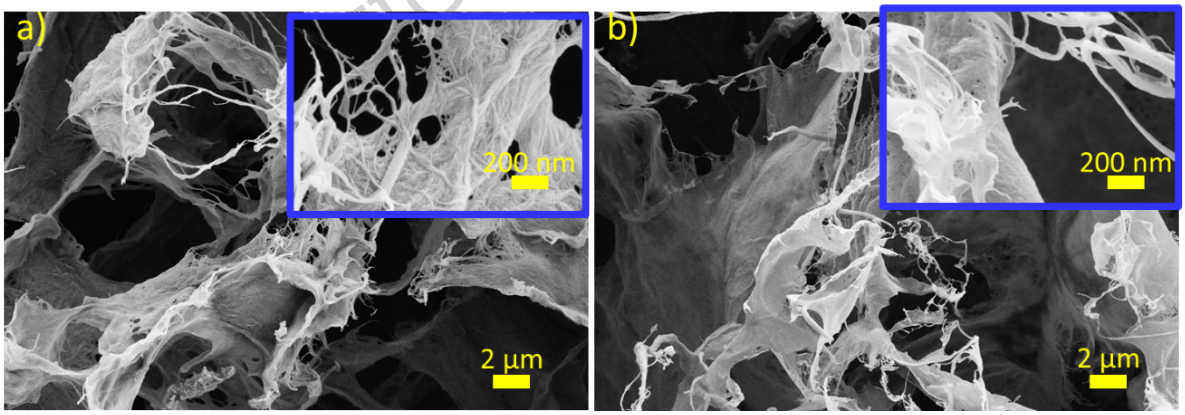

Fig. 3. FESEM micrographs of nanochitin of a) mechanical and b) TEMPO-oxidized.

3.2. Transparency

Figure 4 shows that the apparent transparency of TEMPO-oxidized nanochitin nanopapers is significantly higher than that of mechanical nanopapers (Fig. 4a). The lower transparency in the mechanical nanochitin sample could be due to the non-uniform distribution of fibers and the presence of voids within the structure. These voids increase light scattering and lead to lower transparency. Fukuzumi, et al. [24] demonstrated in their

study that increased porosity and reduced fiber alignment lead to greater light scattering and lower transparency. In contrast, the high transparency of TEMPO-oxidized nanochitin is attributed to its more uniform structure and decreased fiber size. The TEMPO oxidation process produces nanopaper with lower porosity and better fiber alignment. Isogai, et al. [25] found that TEMPO oxidation enhances the transparency of nanopaper by generating thinner fibers and reducing internal porosity.

The transparency of mechanically processed and TEMPO-oxidized nanochitin was evaluated using a UV-Vis spectrophotometer. At a wavelength of 600 nm, TEMPO-oxidized nanochitin exhibited approximately 92% transparency, whereas mechanically processed nanochitin showed only 60% (Fig. 4b). The higher transparency of the TEMPO-oxidized nanochitin is attributed to its homogeneous architecture, smaller nanofiber diameters, and decreased scattering of light owing to its refined microstructural feature [26]. Moreover, light transmission is much smoother in the visible region. This characteristic is a consequence of the chemically modified structure (carboxylate groups introduction) and the increased surface negative charge, which induces electrostatic repulsion between the fibers. This repulsion leads to improved fiber orientation and better matrix formation [27]. In contrast, the lower transparency of the mechanically processed nanochitin is attributed to surface roughness, structural heterogeneity, and enhanced light scattering [25]. This heterogeneity results from the mechanical processing method, which partially damages the internal hydrogen bonds and crystalline structure of the fibers without changing their chemical structure [27]. Due to the high transparency, TEMPO-oxidized nanochitin shows great potential in biodegradable transparent packaging, optical display panels, and protective light coatings. On the other hand, mechanically processed nanochitin with lesser transparency fits towards the requirements of opaque packaging or shading against the plant light. TEMPO-oxidized nanochitin can be prepared into films that could replace common plastic films like polyethylene or PET as biodegradable thin films in the conventional plastic film sector.

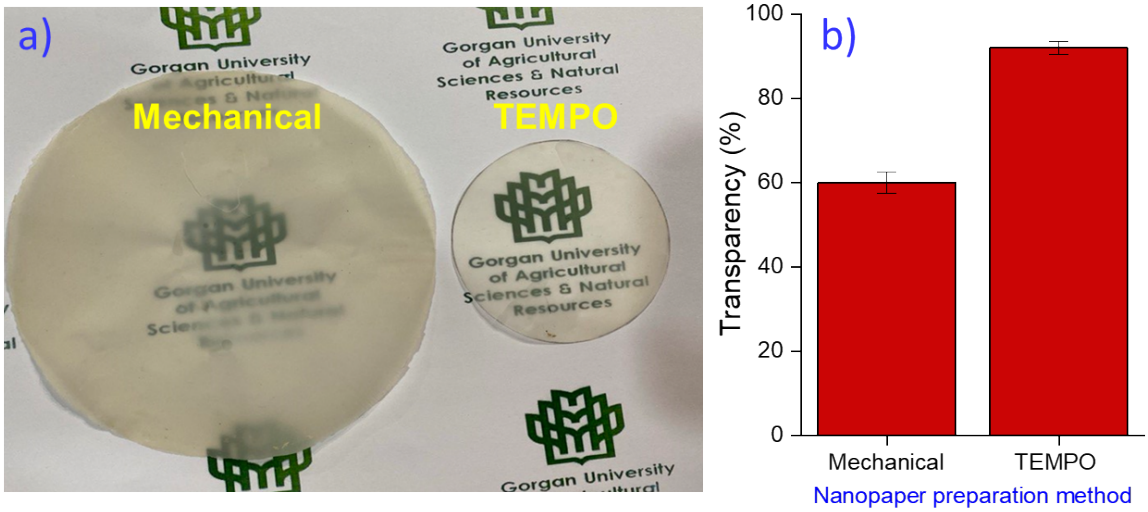

Fig. 4. a) Digital photograph of nanopapers on the Gorgan University of Agricultural Sciences and Natural Resources logo, and b) transparency value of nanopapers.

3.3. X-ray diffraction (XRD)

Figure 5 illustrates the XRD patterns for the mechanocycled and TEMPO-oxidized nanofibers of chitin, and since XRD is a strong tool for probing the crystalline structure of the material, the nanofibers of chitin were confirmed to be crystalline with the diffraction peaks characteristic of the chitin at 2θ values of approximately 9°, 19°, 20°, and 21° for the crystallographic planes of chitin. Mechanical and TEMPO-oxidized chitin nanofiber crystallinity indexes were 91.23% and 91.19%, respectively. The increase in chitin crystallinity after the formation of nanofibers has also been reported in the study of Ye, et al. [28] and confirms that at the nanoscale, the crystalline structure of chitin is more regular in shape and compact, biasing the increasing hardness and strength of chitin.

Notably, the TEMPO-oxidized nanofibers show a weaker and slightly broader peak at around 9° compared to the mechanically processed nanofibers; in the XRD pattern of the TEMPO-oxidized sample, the diffraction peaks may appear relatively shorter or broader due to the reduction in crystallinity induced by oxidation, while additionally exhibiting stronger peaks at around 14°, 20°, and 21°. The presence of extra peaks or shifts in peak positions may indicate potential alterations in the crystal lattice structure resulting from introducing carboxylate groups [29]. Nonetheless, no dramatic differences in the peaks of the two samples in their XRD patterns were noted, implying that the crystalline structure of the chitin is mostly preserved throughout the TEMPO-mediated oxidation procedure [30]. It is important to note that variations in preparation methods, the degree of oxidation, and the presence of impurities can affect the XRD patterns of both mechanically processed and TEMPO-oxidized chitin nanofibers.

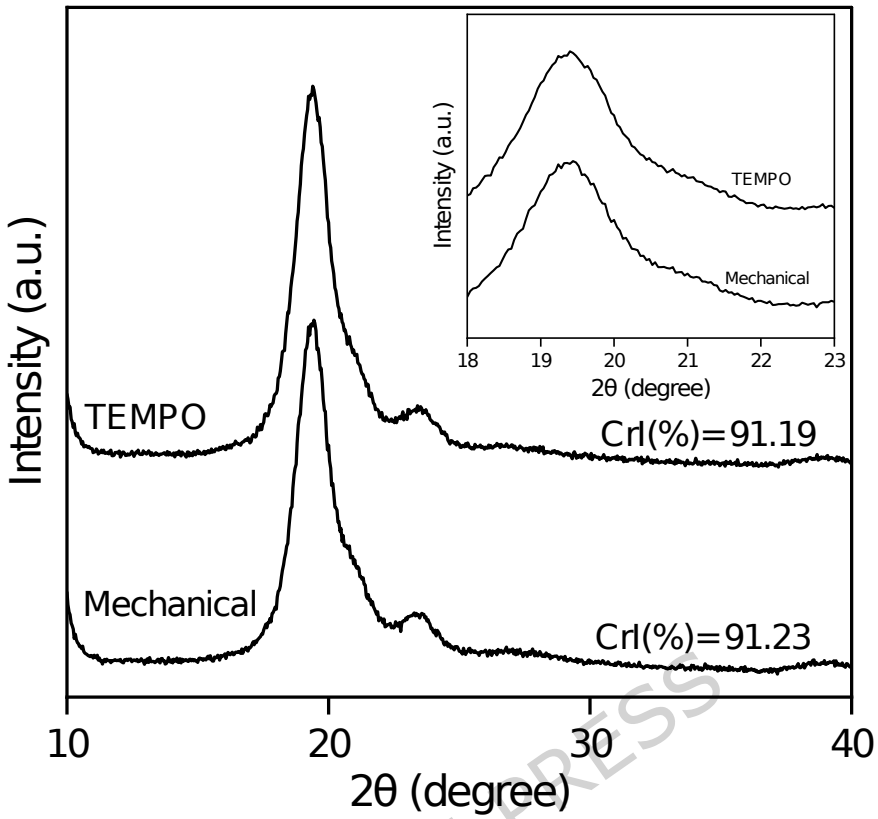

Fig. 5. X-ray diffraction (XRD) pattern of nanochitin nanopapers.

3.4. FTIR

FTIR analysis of the nanopapers reveals distinct absorption peaks that elucidate the chemical structure and modifications resulting from the different processing methods (Fig. 6). The reduced intensity of amine-related bands is in agreement with TEMPO-mediated surface modification, which replaces surface amino functionalities with carboxylate groups, as similarly reported by Salem, et al. [22]. The spectra of both mechanically processed and TEMPO-oxidized nanopapers exhibit characteristic bands around 3400 cm^{-1}, corresponding to O–H stretching vibrations that indicate the presence of hydroxyl groups and extensive hydrogen bonding within the chitin matrix [31]. The peaks near 1630 cm^{-1} and 1560 cm^{-1} are attributed to the amide I (C=O stretching) and amide II (N–H bending) vibrations [12], respectively, which confirm the preservation of the chitin backbone. Other bands, such as those near 1310 cm^{-1} and 1150 cm^{-1}, further reflect CH bending and C–O stretching vibrations, underscoring the chemical complexity of the nanostructured films. FTIR findings demonstrate that while the fundamental chitin structure is maintained in both samples, the TEMPO oxidation process induces specific chemical modifications that enhance the functional properties of the resulting nanopapers.

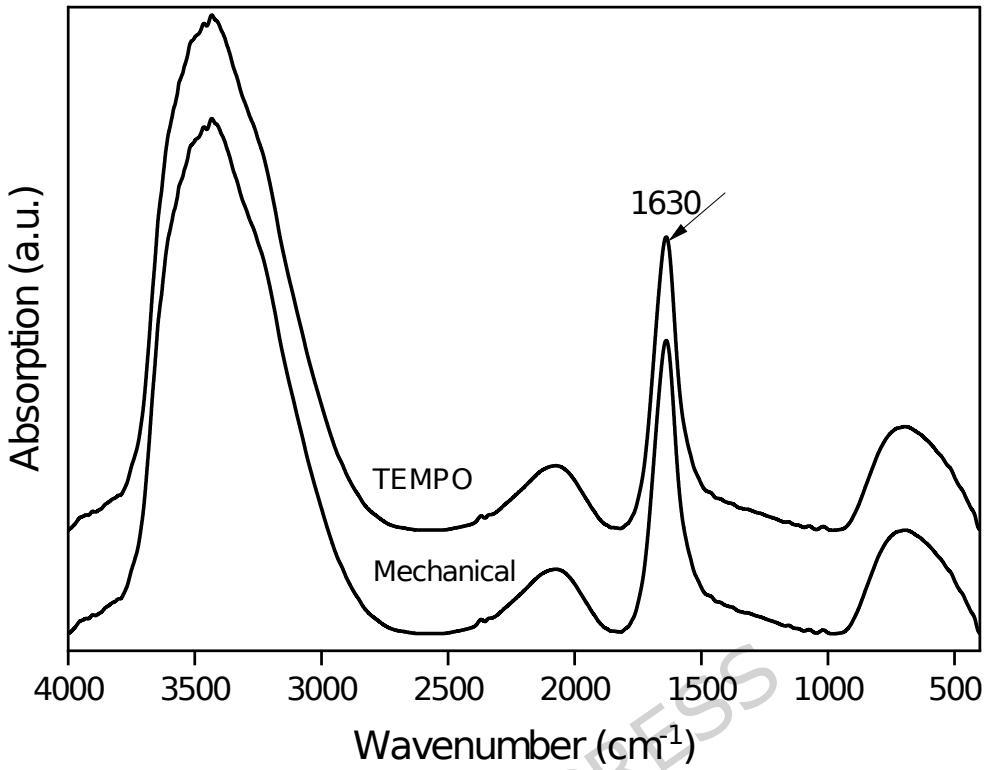

Fig. 6. FTIR spectra of nanochitin nanopapers: a) mechanical and b) TEMPO.

3.5. Mechanical properties

The tensile strength, Young's modulus, and strain of nanopapers made with mechanically processed nanochitin and TEMPO-oxidized nanochitin are shown in Fig. 7. The value of tensile strength for the mechanically processed nanochitin (60.3 MPa) is almost two times higher than that for TEMPO-oxidized nanochitin (33.2 MPa), which may be related to more strong hydrogen bonding of the mechanically processed nanochitin, leading to greater resistance to tensile stresses [32]. In the TEMPO-oxidation process, the introduction of carboxyl groups into the nanochitin structure impairs these hydrogen bonds, which may lead to lower tensile strength [25]. The Young's modulus of the mechanical nanochitin (3.52 GPa) is higher than that of the TEMPO-oxidized nanochitin (2.70 GPa). The higher Young's modulus of mechanical nanochitin indicates higher stiffness and greater resistance to small deformations. This property is very suitable for preparing films that require high structural strength (such as robust packaging or protective layers) [17]. Moreover, this difference also stems from the more ordered crystalline structure of the mechanically processed nanochitin, as during the mechanical milling process, molecular chains are broken and reconstructed into a denser packing, thus increasing the Young's modulus [18]. Whereas TEMPO oxidation disrupts some hydrogen bonds between the chains and reduces the density of the crystalline structure resulting in a lower Young's modulus [27]. The mechanically processed nanopaper exhibits slightly higher crystallinity, which likely contributes to its superior tensile performance. This

is because increased crystallinity enhances inter-fibril hydrogen bonding and load transfer efficiency. These observations are in line with recent findings on the role of nanoscale ordering in polysaccharide materials [33].

The strain of mechanical nanochitin (1.83%) was higher than that of TEMPO-oxidized nanochitin (1.24%). In general, the greater flexibility of the nanochitin structure results in films with thinner thickness and higher specific surface area, which distributes stress better [34]. Although the TEMPO-oxidized chitin exhibited a more uniform fibril distribution, the mechanical properties were lower than those of the mechanically processed nanopaper because the TEMPO treatment introduced carboxylate groups that reduced hydrogen bonding and decreased crystallinity, thereby limiting stress transfer between adjacent nanofibrils. The TEMPO-oxidation process creates defects in the chitin chains that limit the flexibility of the material [27]. TEMPO-oxidized nanochitin, although less flexible, can be well integrated with other materials or used in environments that require chemical interaction due to its specific chemical surface (the presence of carboxyl groups) [12].

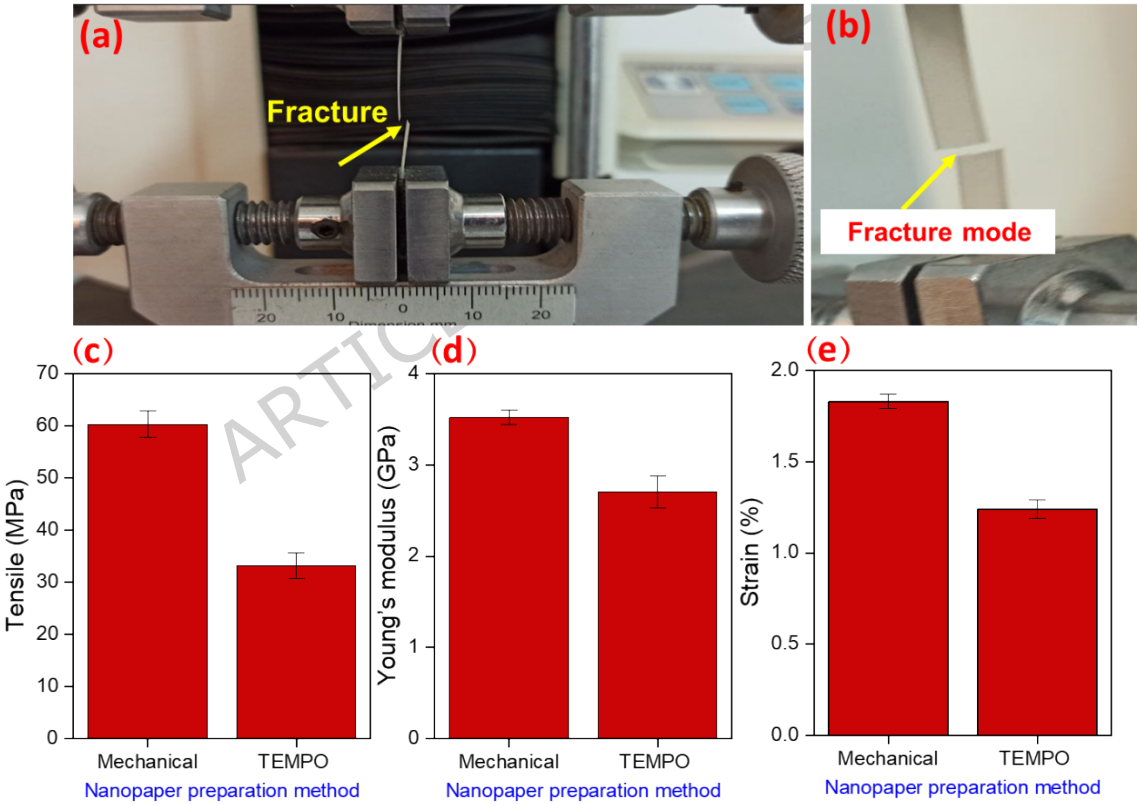

Fig. 7. a) Digital photograph of nanopaper specimen in the tensile test, b) fracture modes, c) tensile test, d) Young's modulus, and e) strain.

4. Conclusions

The study revealed that both nanopapers prepared from chitin nanofibers produced through chemical (TEMPO-oxidized) and mechanical (super disk grinding) processes exhibited high crystallinity values exceeding 90%, with

slightly higher crystallinity in the mechanically processed samples. This structural feature contributed to their greater tensile strength and Young's modulus, which are related to stronger hydrogen bonding and a more compact fibrillar network. In contrast, the TEMPO-oxidized nanopapers showed higher optical transmittance (~92%) and better transparency, attributed to finer fibril diameters and more uniform dispersion. These results indicate that mechanical processing favors the formation of stronger and denser nanopapers, while TEMPO oxidation enhances optical uniformity and light transmittance. Overall, the findings demonstrate that the choice of processing method has a direct influence on the structure and properties of chitin nanopapers, allowing their characteristics to be adjusted according to specific performance requirements.

Declarations

Ethical Approval

Humans or animals are not the subjects of this study. No animals or humans have been studied in this study.

Funding

The authors received no financial support for the research, authorship, and/or publication of this paper.

Competing interests

The authors declare that they have no known competing financial interests or personal relationships that could have appeared to influence the work reported in this paper.

Authors' contributions

Alireza Mohammadlou: Data curation, Software, Resources, Formal analysis, Writing-original draft, supervision, and visualization. **Mohammadreza Dehghani Firouzabadi**: Conceptualization, Methodology, Validation, Investigation, Writing-original draft. **Hossein Yousefi**: Project administration and Methodology. All authors read and approved the final manuscript.

Data availability

The data provided in this study are available to the corresponding author and can be presented on considerable request.

Acknowledgment

The authors are grateful for the support provided by the Gorgan University of Agricultural Sciences and Natural Resources.

References

1 Venugopal, V. Green processing of seafood waste biomass towards blue economy. *Current Research in Environmental Sustainability* **4**, 100164 (2022).

2 Lal, J. *et al.* Diverse uses of valuable seafood processing industry waste for sustainability: a review. *Environmental Science and Pollution Research*, 1–15 (2023).

3 Iber, B. T., Kasan, N. A., Torsabo, D. & Omuwa, J. W. A review of various sources of chitin and chitosan in nature. *Journal of Renewable Materials* **10**, 1097 (2022).

4 Chakravarty, J. & Edwards, T. A. Innovation from waste with biomass-derived chitin and chitosan as green and sustainable polymer: a review. *Energy Nexus* **8**, 100149 (2022).

5 Tan, H. W., Lim, Z. Y. J., Muhamad, N. A. & Liew, F. F. Potential economic value of chitin and its derivatives as major biomaterials of seafood waste, with particular reference to southeast asia. *Journal of Renewable Materials* **10**, 909 (2022).

6 Maraksa, K., Suyotha, W. & Cheirsilp, B. Production of alpha-and beta-chitin, chitosan and protein hydrolysate from seafood processing wastes using an integration of lactic acid and digestive protease from fish viscera as alternative green extraction. *Biocatalysis and Agricultural Biotechnology*, 103496 (2025).

7 Ezekiel Mushi, N., Butchosa, N., Zhou, Q. & Berglund, L. A. Nanopaper membranes from chitin–protein composite nanofibers—structure and mechanical properties. *Journal of applied polymer science* **131** (2014).

8 Zanchetta, E. *et al.* Purification of Cellulose and Chitin Polymers and Other Value-Added Products from the Microalga *Chlorella vulgaris* Using a Green Biorefinery Process. *Fermentation* **11**, 120 (2025).

9 Mohan, K. *et al.* Green and eco-friendly approaches for the extraction of chitin and chitosan: A review. *Carbohydrate Polymers* **287**, 119349 (2022).

10 Aoun, R. B., Trabelsi, N., Abdallah, M., Mourtzinos, I. & Mhamdi, R. Towards a greener future: Exploring the challenges of extraction of chitin and chitosan as bioactive polysaccharides. *Materials Today Communications*, 108761 (2024).

11 Ifuku, S. & Saimoto, H. Chitin nanofibers: preparations, modifications, and applications. *Nanoscale* **4**, 3308–3318 (2012).

12 Liu, L. *et al.* TEMPO-oxidized nanochitin based hydrogels and inter-structure tunable cryogels prepared by sequential chemical and physical crosslinking. *Carbohydrate Polymers* **272**, 118495 (2021).

13 Min, B.-M. *et al.* Chitin and chitosan nanofibers: electrospinning of chitin and deacetylation of chitin nanofibers. *Polymer* **45**, 7137–7142 (2004).

14 Ye, W., Liu, L., Wang, Z., Yu, J. & Fan, Y. Investigation of pretreatment methods for improving TEMPO-mediated oxidation and nanofibrillation efficiency of α-chitin. *ACS Sustainable Chemistry & Engineering* **7**, 19463–19473 (2019).

15 Ye, W., Yokota, S., Fan, Y. & Kondo, T. A combination of aqueous counter collision and TEMPO-mediated oxidation for doubled carboxyl contents of α-chitin nanofibers. *Cellulose* **28**, 2167–2181 (2021).

16 Liu, D., Huang, S., Wu, H. & Zhang, J. Using TEMPO oxidation to tailor deacetylation of carboxyl β-chitin nanofibers from squid pen. *Cellulose* **29**, 8539–8549 (2022).

17 Yousefi, H. *et al.* Comparative study of paper and nanopaper properties prepared from bacterial cellulose nanofibers and fibers/ground cellulose nanofibers of canola straw. *Industrial Crops and Products* **43**, 732–737 (2013).

18 Yousefi, H., Faezipour, M., Nishino, T., Shakeri, A. & Ebrahimi, G. All-cellulose composite and nanocomposite made from partially dissolved micro-and nanofibers of canola straw. *Polymer Journal* **43**, 559–564 (2011).

19 González, I. *et al.* From paper to nanopaper: evolution of mechanical and physical properties. *Cellulose* **21**, 2599–2609 (2014).

20 Fan, Y., Saito, T. & Isogai, A. Preparation of chitin nanofibers from squid pen β-chitin by simple mechanical treatment under acid conditions. *Biomacromolecules* **9**, 1919–1923 (2008).

21 French, A. D. Idealized powder diffraction patterns for cellulose polymorphs. *Cellulose* **21**, 885–896 (2014).

22 Salem, K. S., Starkey, H. R., Pal, L., Lucia, L. & Jameel, H. The topochemistry of cellulose nanofibrils as a function of mechanical generation energy. *ACS Sustainable Chemistry & Engineering* **8**, 1471–1478 (2019).

23 Chen, R., Huang, W.-C., Wang, W. & Mao, X. Characterization of TEMPO-oxidized chitin nanofibers with various oxidation times and its application as an enzyme immobilization support. *Marine Life Science & Technology* **3**, 85–93 (2021).

24 Fukuzumi, H., Saito, T., Iwata, T., Kumamoto, Y. & Isogai, A. Transparent and high gas barrier films of cellulose nanofibers prepared by TEMPO-mediated oxidation. *Biomacromolecules* **10**, 162–165 (2009).

25 Isogai, A., Saito, T. & Fukuzumi, H. TEMPO-oxidized cellulose nanofibers. *Nanoscale* **3**, 71–85 (2011).

26 Fang, Z. *et al.* Novel nanostructured paper with ultrahigh transparency and ultrahigh haze for solar cells. *Nano letters* **14**, 765–773 (2014).

27 Saito, T., Kimura, S., Nishiyama, Y. & Isogai, A. Cellulose nanofibers prepared by TEMPO-mediated oxidation of native cellulose. *Biomacromolecules* **8**, 2485–2491 (2007).

28 Ye, W. *et al.* Comparison of cast films and hydrogels based on chitin nanofibers prepared using TEMPO/NaBr/NaClO and TEMPO/NaClO/$NaClO_2$ systems. *Carbohydrate Polymers* **237**, 116125 (2020).

29 Sajomsang, W. & Gonil, P. Preparation and characterization of α-chitin from cicada sloughs. *Materials Science and Engineering: C* **30**, 357–363 (2010).

30 Mushi, N. E., Utsel, S. & Berglund, L. A. Nanostructured biocomposite films of high toughness based on native chitin nanofibers and chitosan. *Frontiers in Chemistry* **2**, 99 (2014).

31 Hossin, M. A., Al Shaqsi, N. H. K., Al Touby, S. S. J. & Al Sibani, M. A. A review of polymeric chitin extraction, characterization, and applications. *Arabian Journal of Geosciences* **14**, 1870 (2021).

32 Sehaqui, H., Salajková, M., Zhou, Q. & Berglund, L. A. Mechanical performance tailoring of tough ultra-high porosity foams prepared from cellulose I nanofiber suspensions. *Soft Matter* **6**, 1824–1832 (2010).

33 Salem, K. S. *et al.* Comparison and assessment of methods for cellulose crystallinity determination. *Chemical Society Reviews* **52**, 6417–6446 (2023).

34 Habibi, Y., Lucia, L. A. & Rojas, O. J. Cellulose nanocrystals: chemistry, self-assembly, and applications. *Chemical reviews* **110**, 3479–3500 (2010).